THE JOURNAL OF BIOLOGICAL CHEMISTRY
Vol. 276, No. 25, Issue of June 22, pp. 22868–22874, 2001

Printed in U.S.A.

Calcium Transients in 1B5 Myotubes Lacking Ryanodine Receptors Are Related to Inositol Trisphosphate Receptors*

Received for publication, January 5, 2001, and in revised form, April 3, 2001
Published, JBC Papers in Press, April 11, 2001, DOI 10.1074/jbc.M100118200

Manuel Estrada, Cesar Cárdenas, José L. Liberona, M. Angélica Carrasco, Gregory A. Mignery‡, Paul D. Allen§, and Enrique Jaimovich¶

From the Instituto de Ciencias Biomédicas, Facultad de Medicina, Universidad de Chile, Casilla 70005, Santiago 6530499, Chile, ‡Department of Physiology, Loyola University, Chicago, Illinois 60153, and §Department of Anesthesia, Brigham and Women's Hospital, Boston, Massachusetts, 02115

Potassium depolarization of skeletal myotubes evokes slow calcium waves that are unrelated to contraction and involve the cell nucleus (Jaimovich, E., Reyes, R., Liberona, J. L., and Powell, J. A. (2000) *Am. J. Physiol.* 278, C998–C1010). Studies were done in both the 1B5 (Ry53−/−) murine "dyspedic" myoblast cell line, which does not express any ryanodine receptor isoforms (Moore, R. A., Nguyen, H., Galceran, J., Pessah, I. N., and Allen, P. D. (1998) *J. Cell Biol.* 140, 843–851), and C_2C_{12} cells, a myoblast cell line that expresses all three isoforms. Although 1B5 cells lack ryanodine binding, they bind tritiated inositol (1,4,5)-trisphosphate. Both type 1 and type 3 inositol trisphosphate receptors were immuno-located in the nuclei of both cell types and were visualized by Western blot analysis. After stimulation with 47 mM K^+, inositol trisphosphate mass raised transiently in both cell types. Both fast calcium increase and slow propagated calcium signals were seen in C_2C_{12} myotubes. However, 1B5 myotubes (as well as ryanodine-treated C_2C_{12} myotubes) displayed only a long-lasting, non-propagating calcium increase, particularly evident in the nuclei. Calcium signals in 1B5 myotubes were almost completely blocked by inhibitors of the inositol trisphosphate pathway: U73122, 2-aminoethoxydiphenyl borate, or xestospongin C. Results support the hypothesis that inositol trisphosphate mediates slow calcium signals in muscle cell ryanodine receptors, having a role in their time course and propagation.

Depolarization-induced calcium release in skeletal muscle is generally detected as a fast process mediated by dihydropyridine receptors in the T-tubule membrane and ryanodine receptors (RyR)[1] in the sarcoplasmic reticulum (1–4). We previously found evidence for at least two identifiable calcium signals (5, 6) in skeletal muscle cells in cultures exposed to high external potassium, which suggests that there are at least two calcium release systems that respond to the depolarization signal. The two signals were called the fast and slow waves. We were also able to observe fluorescence heterogeneity during slow waves, corresponding to two separate processes: first, a more rapid increase in fluorescence (the "slow-rapid" wave) that propagates through both nuclei and cytosol regions; second, a slower component of increased fluorescence (the "slow-slow" wave), which is seen only in the nuclear region.

The fact that the cell does not contract during either part of the slow wave indicates that the overall cytosolic calcium concentration remains below the contraction threshold and that the high fluorescence areas that we see must be highly compartmentalized, most probably in the nuclear region. As expected, high concentrations of ryanodine eliminated the initial rapid calcium increase associated with contraction, and interestingly, it also eliminated the first or slow-rapid cytosolic propagation as well. However the second slow calcium rise phase was preserved. This suggests that a ryanodine-sensitive calcium pool is involved in the mechanism of propagation of the slow-rapid Ca^{2+} wave through the cytosol. The apparently different intracellular distributions of receptors, RyR in the sarcoplasmic reticulum membranes and inositol 1,4,5-trisphosphate receptors (IP_3R), at least in some developmental stages, concentrated in membranes associated with the nuclei (7–9), points to the presence of two separate calcium release systems. We proposed that the role for the IP_3R could be to modulate cytosolic calcium concentrations within the appropriate levels, sub-cellular regions, and time scale required to activate nuclear calcium release. Slow calcium signals in these cells appear to be mediated by IP_3 receptors and are likely to control phosphorylation cascades involved in regulation of gene expression.[2] The aim of the present work was to determine the definitive role of RyRs, if any, in either component of the slow release process. To this aim, we compared the calcium signals in dyspedic muscle cells (1B5), which do not express any of the RyR isoforms and lack excitation-contraction (E-C) coupling (10–17) to C_2C_{12} cells, which have wild type calcium signals.

MATERIALS AND METHODS

Cell Cultures—Myoblasts of the immortalized dyspedic mouse myoblast cell line 1B5 (3) and the C_2C_{12} myoblast line (American Type Culture Collection, Manassas, VA) were cultivated in Dulbecco's modified Eagle's medium (1 g of glucose/liter), 10% heat-inactivated fetal calf serum, and 10% bovine serum (all Life Technologies, Inc.) in gelatin-covered dishes at 37 °C in 5% CO_2. The serum was reduced to 2% horse serum after 2 days to induce cell maturation and fusion, and cells were studied 5–7 days after differentiation was initiated.

Intracellular Calcium—For intracellular calcium measurements at single-cell level, the myoblasts were cultured on glass coverslips to reach 80% confluence and then differentiated into myotubes by withdrawal of growth factors. Calcium images were obtained from myotubes

* This work was supported by European Economic Community Grant CI1-CT94-0129, Fondo Nacional de Ciencia y Tecnologia Grants 8980010 (to E. J.) and 2000055 (to M. E.), and National Institutes of Health Grant R01AR43140 (to P. D. A).The costs of publication of this article were defrayed in part by the payment of page charges. This article must therefore be hereby marked "*advertisement*" in accordance with 18 U.S.C. Section 1734 solely to indicate this fact.

¶ To whom correspondence should be addressed: Casilla 70005, Santiago 6530499, Chile. Tel.: 56-2 678–6311; Fax: 56-2 7776916; E-mail: ejaimovi@machi.med.uchile.cl.

[1] The abbreviations used are: RyR, ryanodine receptor; IP_3 inositol 1,4,5-trisphosphate; IP_3R, IP_3 receptor; MES, 4-morpholineethanesulfonic acid.

[2] J. A. Powell, M. A. Carrasco, D. S. Adams, B. Drouet, J. Rios, M. Müller, M. Estrada, and E. Jaimovich, unpublished information.

that were loaded with the fluorescence calcium dye fluo-3-acetoximethylester (fluo-3AM; Molecular Probes, Eugene, OR) using an inverted confocal microscope (Carl Zeiss Axiovert 135 M-LSM Microsystems). Alternatively we observed calcium transients with an epifluorescence microscope (Olympus) equipped with a cooled CCD camera and image acquisition system (Spectra Source MCD 600). Myotubes were washed three times with Krebs buffer (145 mM NaCl, 5 mM KCl, 2.6 $CaCl_2$, 1 mM $MgCl_2$, 10 mM Hepes-Na, 5.6 mM glucose, pH 7.4) to remove serum and loaded with 5.4 μM fluo-3 (coming from a stock in pluronic acid, 20% Me_2SO) for 30 min at room temperature. After loading, myotubes were washed for 10 min to allow the deesterification of the dye and used within 2 h. The coverslips were mounted in a 1-ml capacity plastic chamber and placed in the microscope for fluorescence measurements. After excitation with a 488-nm wavelength argon laser beam or filter system, the fluorescence images were collected every 0.4–2.0 s and analyzed frame by frame with the data acquisition program of the equipment. A PlanApo 60X (NA 1.4) objective lens was used. In most of the acquisitions, the image dimension was 512 × 120 pixels. Intracellular calcium was expressed as a percentage of fluorescence intensity relative to basal fluorescence (a value stable for at least 5 min in resting conditions). The increase in fluorescence intensity of fluo-3 is proportional to the rise in intracellular calcium level (18). For experiments using inhibitors, U-72133 (Sigma), 2-aminoethoxydiphenyl borate (Aldrich), xestospongin C (Calbiochem), and ryanodine (Sigma) were used.

Digital Image Processing—Elimination of out-of-focus fluorescence was performed using both the "no-neighbors" deconvolution algorithm and Castleman's (19) PSF (point spread function) theoretical model, as has been described previously (20). To quantify fluorescence, the summed pixel intensity was calculated on the section delimited by a contour. As a way of increasing efficiency of these data manipulations, action sequences were generated. To avoid the possible interference in the fluorescence by high potassium solution effects on the cellular volume, the area of fluorescent cell was determined by image analysis using adaptive contour and then creating a binary mask, which was compared with its bright-field image.

Binding of [^{3}H]IP_3 and [^{3}H]Ryanodine—Radioligand binding assay for [^{3}H]IP_3 was determined as described (9). Briefly, confluent plates of C_2C_{12} and dyspedic mouse cell lines 5–7 days after withdrawal of serum were washed three times with phosphate-buffered saline and homogenized with an ultrasonic homogenizer for 10–15 s. They were then incubated in a medium that contained 50 mM Tris-HCl, pH 8.4, 1 mM EDTA, 1 mM 2-mercaptoethanol, and different concentrations (10–200 nM) of [^{3}H]IP_3 (D-*myo*-[2-^{3}H]IP_3, specific activity 21.0 Ci/mmol, PerkinElmer Life Sciences, 800–1000 cpm/pmol) to 4 °C for 30 min. After incubation, the reaction was stopped by centrifugation at 10,000 × *g* for 10 min (Heraus Biofuge 15R), the supernatant was aspired, and the pellets were washed with phosphate-buffered saline and dissolved in NaOH (1 M) to measured the radioactivity. The nonspecific binding was determined in the presence of 2 μM IP_3 (Sigma). [^{3}H]Ryanodine binding was measured in C_2C_{12} and dyspedic mouse cell homogenates as described (21). The incubation medium contained 0.5 M KCl, 0.1 mM $CaCl_2$, 20 mM Hepes-Tris, pH 7.1, and 1 mM 5′-adenylylimidodiphosphate or 5 mM adenosine trisphosphate. The samples were incubated with [^{3}H]ryanodine (5–100 nM) for 90 min at 37 °C in the presence or absence of cold ryanodine (10 μM) for nonspecific binding.

Western Blots—Homogenate proteins were resolved in 7% SDS-polyacrylamide electrophoresis gels and transferred to nitrocellulose membranes for 2 h at 0.2 A. Primary antibody incubations using dilutions of 1:1000 of antibodies against either type 1 (Affinity Bioreagents) or type 3 (Transduction Laboratories) IP_3 receptor were carried out at 4 °C overnight. After incubation with horseradish peroxidase-conjugated secondary antibodies for 1.5 h, the membranes were developed by enhanced chemiluminescence according to the manufacturer's instructions. After scanning the films, a densitometry analysis of the bands was performed with the Scion Image program from NIH.

Immunocytochemistry—Myotubes grown on coverslips were fixed in iced methanol, blocked in phosphate-buffered saline containing 1% bovine serum albumin and 10% goat serum for 30 min and incubated with primary antibodies at 4 °C overnight. The primary antibodies obtained from commercial sources were raised against anti-ryanodine receptor (monoclonal; Affinity Bioreagents) and anti-type 1 IP_3R (polyclonal; Affinity Bioreagents). Anti-type-3 IP_3R antibody was raised in rabbits against a peptide corresponding to the carboxyl-terminal 16 amino acids of the rat type-3 IP_3R cDNA (CRRQRLGFVDVQNCMSR) (22). The antibody used in this study was affinity-purified using the immunogenic peptide. The cells were then washed five times with phosphate-buffered saline/bovine serum albumin and incubated with the appropriate goat anti-mouse or goat anti-rabbit secondary antibodies for 1 h at room temperature. After washing three more times, the coverslips were mounted in 90% glycerol, 0.1 M Tris, pH 8.0, and 5 mg/ml *p*-phenylendiamine to retard photobleaching. The samples were evaluated in a scanning confocal microscope and phase contrast microscope and documented through computerized images. In most cases a nuclear staining was carried out with #33342 Hoeschst (Polyscience Inc., Warrington, PA) either before fixing or added to the secondary antibody preparation. Primary antibodies were used in 1:100 to 1:25 dilutions and label displacement with the antigenic peptide was used as a test for specificity.

Measurements of IP_3 Mass Changes in Response to High External Potassium—Myotubes were rinsed and preincubated at room temperature for 20 min with a "resting solution" of the following composition: 58 mM NaCl, 4.7 mM KCl, 3 mM $CaCl_2$, 1.2 mM $MgSO_4$, 0.5 mM EDTA, 60 mM LiCl, 10 mM glucose, and 20 mM Hepes, pH 7.4. Next the cells were stimulated, replacing this solution by high potassium solution. At the times indicated, the reaction was stopped by rapid aspiration of the stimulating solution, the addition of 0.8 M ice-cold perchloric acid, and freezing with liquid nitrogen. Samples were allowed to thaw, and cell debris was spun down for protein determination. The supernatant was neutralized with a solution 2 M KOH, 0.1 M MES, and 15 mM EDTA. The neutralized extracts were frozen until required for IP_3 determination. IP_3 mass measurements were carried out by radioreceptor assay (23). Briefly, a crude rat cerebellum membrane preparation was obtained after homogenization in 50 mM Tris-HCl, pH 7.7, 1 mM EDTA, 2 mM β-mercaptoethanol and centrifugation at 20,000 × *g* for 15 min. This procedure was repeated 3 times, suspending the final pellet in the same solution plus 0.3 M sucrose and freezing it at −80 °C until use. The membrane preparation was calibrated for IP_3 binding with 1.6 nM [^{3}H]IP_3 (DuPont) and 2–120 nM cold IP_3 (Sigma) carrying out the sample analysis in a similar way but adding an aliquot of the neutralized supernatant instead of cold IP_3. [^{3}H]IP_3 radioactivity remaining bound to the membranes was measured in a Beckman LS-6000TA liquid scintillation spectrometer (Beckman Instruments). Cell number was counted in a hemocytometer using trypan blue exclusion to identify living cells before plating.

Statistics—All data are expressed as mean ± S.D. Differences between basal and post-stimulated points were determined using a paired Student's *t* test. $p < 0.05$ was considered statistically significant.

RESULTS

Intracellular Calcium Signals—Confocal microscopy was used to investigate fluo-3 fluorescence in both a RyR-expressing mouse muscle cell line (C_2C_{12}) and in dyspedic cells (1B5) in response to potassium depolarization. A typical effect of high potassium solution (47 mM K^+) on intracellular calcium in C_2C_{12} cells (Fig. 1*A*) consists of a fast (reaching the peak in less than 1 s) increase of fluo-3 fluorescence in the entire cell (n = 54 of 63); fluorescence slowly decreased during the next few seconds. After the first signal began to decline, a second, smaller signal was evident at about 10–20 s in 48% of the cells observed (n = 26). This signal usually propagates along a region of the cell, and fluorescence in some nuclei continues to increase after the wave passes them. The analysis of this particular cell allowed measurements of a given calcium signal in different regions of the myotube in order to study these phenomena (see below). The response seen is similar to the calcium transients described in cultured primary rat (5, 6) or mice[2] myotubes. Nuclear region signals appear to have a relative fluorescence change higher than the cytoplasmic signals, probably because fluo-3 is concentrated in the nucleoplasm (6). Myotubes from the dyspedic (1B5) skeletal muscle cell line, which lacks ryanodine receptors, also displayed intracellular calcium increases upon K^+ stimulation, but the kinetic pattern of this signal was different from that of their "normal" counterpart (Fig. 1*B*). As expected in dyspedic myotubes, the fast calcium signal was not present. However, a slow increase of calcium in the nuclei was apparent several seconds (mean time 8.2 ± 4.6 s range 2–18 s) after K^+ stimulation. No propagation of this signal in the cytoplasm was evident. A total of 57 independent experiments using K^+ were recorded in dyspedic myotubes; 43 of them (75%) demonstrated a significant slow

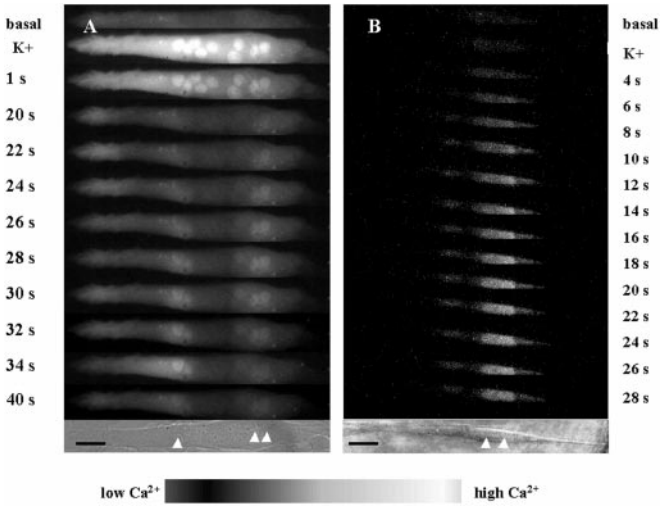

FIG. 1. **Effects of K^+ depolarization on muscle cell lines.** *A*, a series of fluo-3 fluorescence images in C_2C_{12} taken at the times indicated before and after depolarization with 47 mM K^+. Basal fluorescence is shown at the top of the *panel*; the next image was taken immediately after the bath solution was quickly changed to 47 mM potassium (K^+). This solution remained in the bath through the whole record, the following images were acquired every 1 s, a fast and transient increase in intracellular calcium in the myotubes is observed. *B*, a series of fluo-3 fluorescence images in 1B5 cells; potassium (47 mM) addition is indicated. Note that in these cells the rapid calcium increase was not produced; however, a slow increase in both cytoplasmic and nucleoplasmic calcium concentration was evident. The bottom image of each *panel* represents the bright-field image of the cell; distinct nuclei are pointed out by *arrows*. *Calibration bar*, 20 μm.

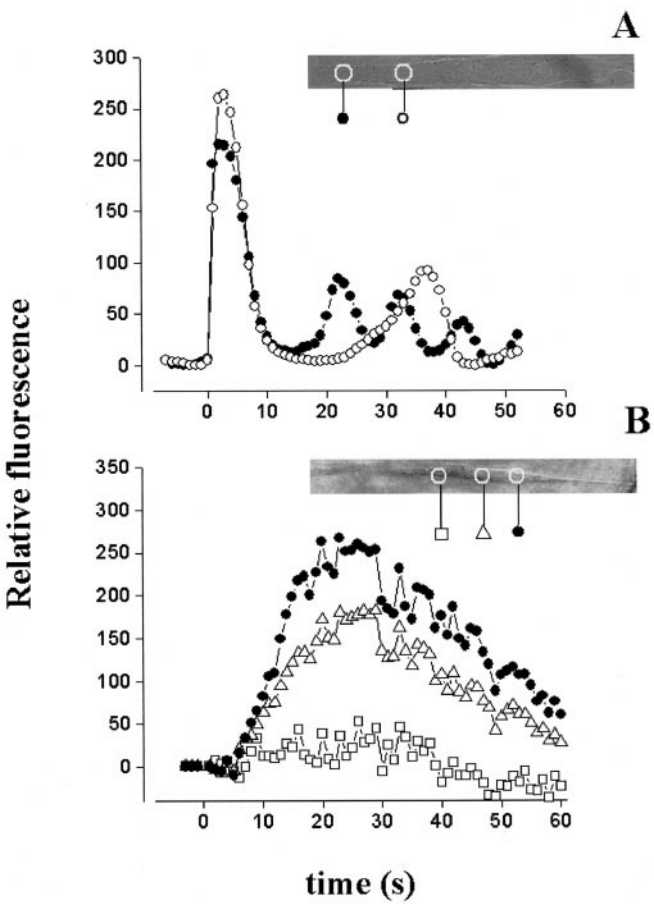

FIG. 2. **Analysis of calcium signals in muscle cell lines.** *A*, the relative fluorescence change (ratio between the fluorescence difference, stimulated minus basal, and the basal value) as a function of time is shown for three different areas in a C_2C_{12} myotube. Two of the areas (*filled symbols*) delimited cell nucleus, and one of the areas (*open squares*) delimited nuclei free cytosol. The three regions measured were the same size. The fast calcium rise was evident in this cell, and a distinct shoulder in the fluorescent signal indicates a delayed onset of fluorescence in a nucleus. *B*, relative nuclear fluorescence changes in two adjacent nuclei (*filled circles*, *open triangles*) and a nucleus free cytosol region (*open squares*) were delimited, and the intensity of all pixels inside these was quantified for each image of the acquired series. Note both the delay in the onset of the signal and the fact that the nuclear fluorescence peak in both nuclei is synchronic.

calcium rise in the nuclear region. It is interesting to note also a difference in duration of the slow calcium signal; the mean duration of Ca^{2+} increase in C_2C_{12} cells was 11.5 ± 6.0 s (range 2–26 s), whereas in dyspedic cells, the mean duration was significantly higher (27.8 ± 13.8 s range 8–42 s; $p < 0.05$).

In a more detailed study of the intracellular calcium increases produced by potassium stimulation in both cell lines, the relative changes in the fluorescence of a cell are displayed as a function of time. In Fig. 2*A*, the series of fluorescence images of a multinucleated C_2C_{12} myotube shown in Fig. 1*A* was analyzed; two different regions of equivalent areas of cytosol containing "responsive" or "unresponsive" nuclei were delimited. Within each contour, the summed intensity of all pixels in each image of the sequence was calculated (20). The fluorescence intensity of all pixels inside the pre-established contour was quantified for each of the images of the acquired series. When the time course of relative fluorescence for C_2C_{12} cells is analyzed (Fig. 2*A*), it is evident that the signal has at least two components. Fast fluorescence rise occurred simultaneously in both areas selected, indicating a very fast, propagated signal that spanned the whole cell in less than 1 s and slowly declined. When we analyze two sections separated by 33 μm, it can be seen that fluorescence rises in both areas at the same time (fast component). However, the slow component occurred as an oscillation, starting earlier in the left-side region (*filled circles*) and then propagated to the right (*empty circles*). As a distinct nucleus fluoresced in the right-hand region (see Fig. 2*A*, inset), it is possible to notice a shoulder in the curve, indicating the presence of both a faster (smaller) and a delayed component in this signal (*empty circles*). A similar analysis for dyspedic myotubes was also performed (Fig. 2*B*). 1B5 cells show a delayed, not propagated component of calcium rise that lasted longer than those of C_2C_{12} cells and was clearly higher in nuclear than in cytosolic regions (compare the intensity of the signal in two areas containing nuclei with that of a cytosolic area, Fig. 2*B*). In another subset of experiments, we tested a possible role of calcium influx on K^+-activated Ca^{2+} transients with confocal imaging. To minimize Ca^{2+} entry into myotubes, the experiments were performed in a low external Ca^{2+} solution containing 96 mM NaCl, 5 mM $MgCl_2$, 2 mM KCl, 5 mM Hepes, 0.5 mM EGTA. In seven independent experiments each of the calcium transients were clearly visible in both C_2C_{12} and 1B5 cells, and the spatial and temporal pattern of those signals were similar to those obtained in normal external calcium (data not shown).

Use of Inhibitors of the IP_3 Pathway—To identify the calcium release systems involved in these signals, we measured calcium signals in both 1B5 and C_2C_{12} cells in the presence of known inhibitors of IP_3-mediated processes. In 1B5 cells (Fig. 3), the calcium rise was either completely blocked or greatly inhibited in the presence of 10 μM phospholipase C inhibitor U73122 (5 out of 6 experiments). The same happened for the slow part of the signal in C_2C_{12} cells (not shown). 100 μM xestospongin C, an IP_3 receptor blocker (24), also almost completely inhibited the calcium rise in 6 out of 7 experiments with 1B5 cells. Finally, as was shown by Powell *et al.*[2] in primary cultures, 50 μM cell-permeant modulator of the IP_3-signaling 2-aminoethoxydiphenyl borate (25) also inhibited the slow calcium sig-

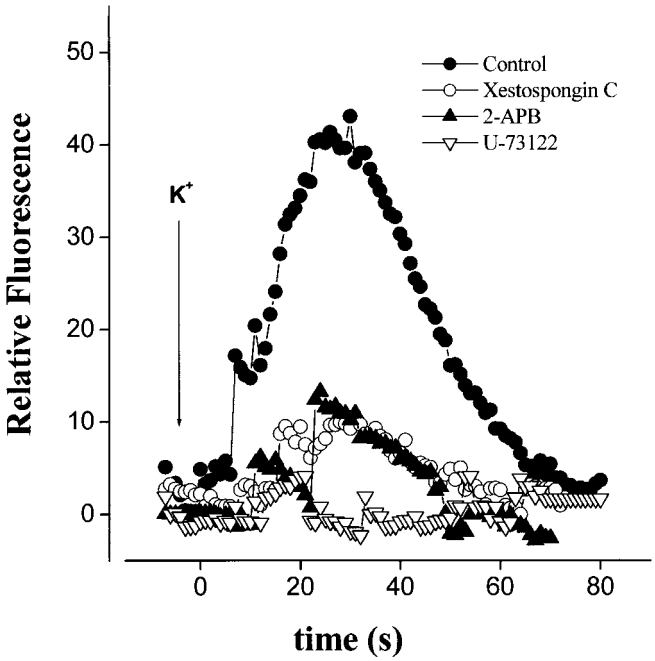

FIG. 3. **Effect of inhibitors of IP_3 pathway on calcium signal in 1B5 myotubes.** Cells were preincubated for 30 min with U73122 (10 μM), 2-aminoethoxydiphenyl borate (*2APB*) (50 μM), or xestospongin C (100 μM), as indicated for each curve before inducing a calcium signal by high potassium depolarization (*arrow*). Note that the three different inhibitors of IP_3-mediated process almost completely blocked the slow calcium increase in 1B5 myotubes. A relatively small increase in calcium was chosen for the control cell in this case.

nal in both cell lines (9 out of 12 experiments) but did not affect the fast calcium rise in C_2C_{12} cells (not shown).

C_2C_{12} Incubated with Ryanodine—When C_2C_{12} cells were previously incubated with 20 μM ryanodine, the fast rise after potassium depolarization was completely abolished (Fig. 4), and a long-lasting increase of calcium fluorescence (mean duration 28 ± 6 s) was evident in the whole cell after a 6-s delay. Note that fluorescence intensity was particularly high at the level of the cell nuclei. It is also important to note in this case the complete lack of slow propagation of the signal, all nuclear fluorescence increasing at about the same time (Fig. 4).

[^{3}H]Ryanodine and [^{3}H]IP_3 Binding—The presence of ryanodine receptor/calcium release channels (RyR channels) in C_2C_{12} and 1B5 skeletal myotubes was studied using a radioligand assay. In C_2C_{12} cells, [^{3}H]ryanodine binding as a function of [^{3}H]ryanodine concentration was hyperbolic (Fig. 5*A*). The Scatchard analysis for the specific binding component (*inset*, Fig. 5*A*) was fitted to a single family of receptors, with a high maximal binding capacity (B_{max} = 0.88 pmol/mg of protein). [^{3}H]Ryanodine binding to C_2C_{12} myotubes is similar to that described for other skeletal muscle myotubes (6, 9, 26). On the other hand, under identical assay conditions, no specific [^{3}H]ryanodine binding could be detected in dyspedic myotubes (1B5 cells), since no difference between total and nonspecific binding was found (Fig. 5*B*). This confirms the previously published results for this cell line (13). A second family of calcium release channels known to be targeted to the nucleus corresponds to inositol 1,4,5- trisphosphate receptors (27, 28). Expression of IP_3Rs in C_2C_{12} as well as 1B5 myotubes was determined by [^{3}H]IP_3 binding to myotube homogenates of C_2C_{12} and 1B5 cells, respectively (Figs. 5, *C* and *D*). A saturating (specific) binding curve for [^{3}H]IP_3 was found in both cell lines. The Scatchard analysis for the specific binding component was fitted to a single family of receptors, with a high maximal binding capacity. Similar K_d values were found in 1B5 and C_2C_{12} myotubes, 61.8 ± 16.3 and 60.1 ± 22.2 nM, respectively, and the total amount of IP_3 receptors (B_{max}) was the same in both cell types (3.12 *versus* 2.8 pmol/mg of protein, respectively).

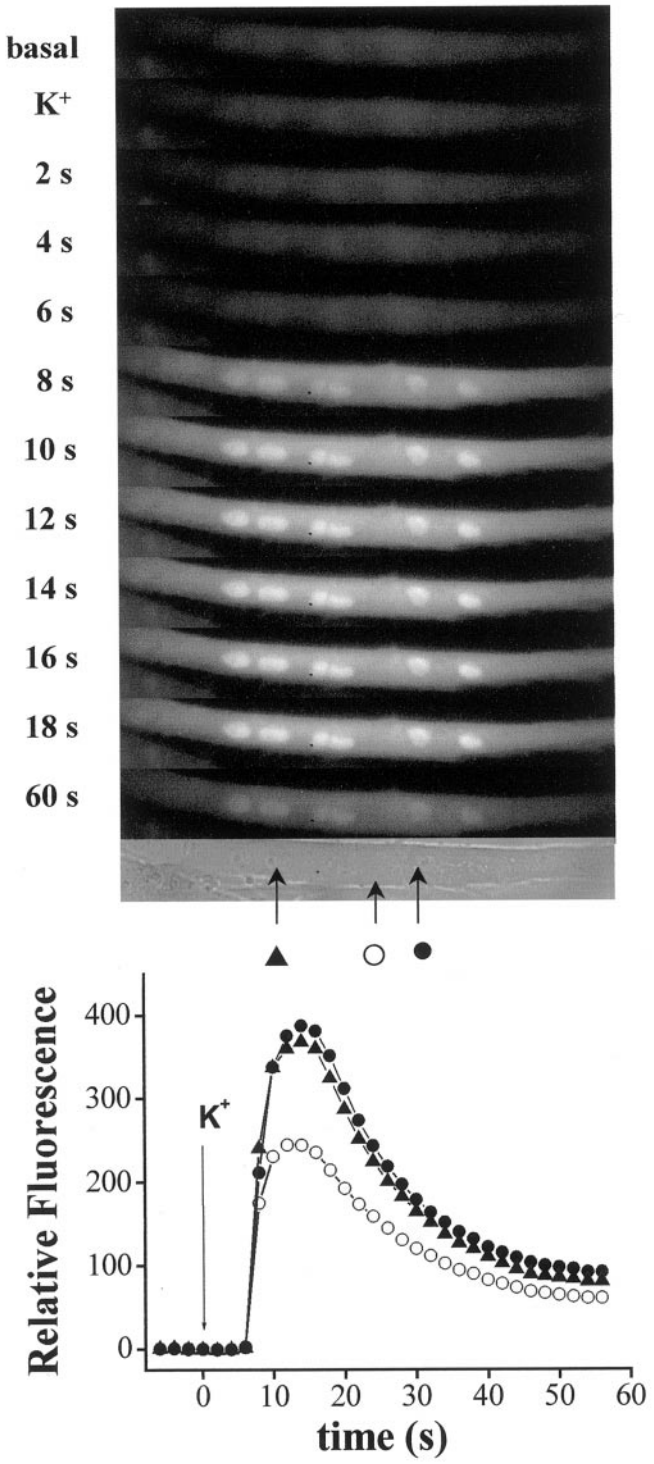

FIG. 4. **Calcium transient in C_2C_{12} muscle cells.** Effect of ryanodine on fast and slow signals. *Upper panel*, a set of images taken every 2 s in a myotube incubated for 30 min with 20 μM ryanodine. No fast signal is apparent; a delayed slow signal appears by 8 s. After several seconds, the central part of the myotube became clearly fluorescent, but the propagation of the signal was not apparent. Total length of the myotube segment, 208 μm. *Lower panel*, time course of relative fluorescence in two different nuclei (*filled symbols*) 97 μm apart and in a cytosol region (*open circles*) in between them. The three regions measured were the same size and are indicated by *arrows* in the *center panel*.

Western Blot Analysis—The presence of different IP_3R isoforms was investigated in C_2C_{12} and 1B5 cell myotubes by

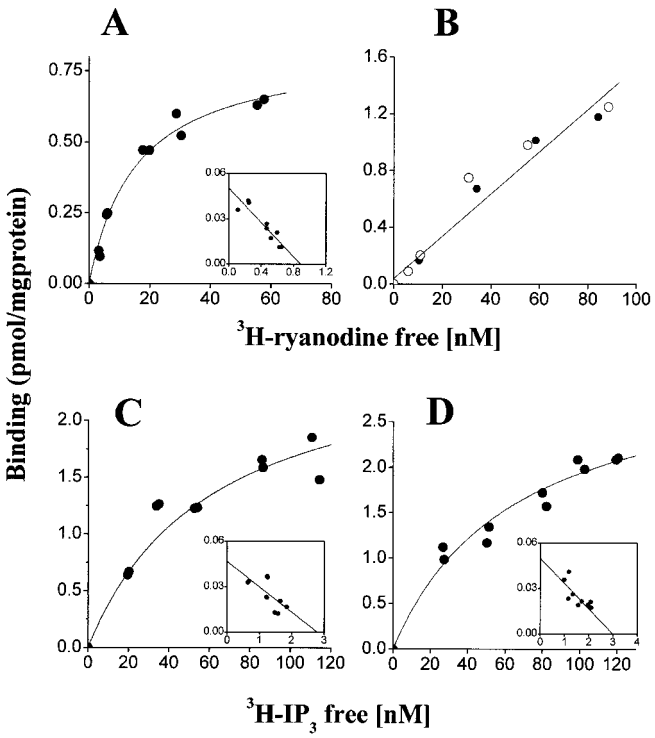

FIG. 5. **[^{3}H]IP$_3$ and [^{3}H]ryanodine binding in C_2C_{12} and 1B5 cells.** *A*, the microsomal membrane fraction of C_2C_{12} cells shows specific [^{3}H]ryanodine binding (nonspecific binding, not shown, was subtracted to all points); data was fitted to a K_d of 17.7 ± 2.9 nM and a maximal binding capacity of 0.88 pmol/mg of protein. Nonspecific binding was measured in the presence of 10 μM ryanodine. *B*, [^{3}H]ryanodine binding to 1B5 cell homogenates. The specific ryanodine binding component is absent. No differences were found between total and nonspecific curves. *C*, a microsomal membrane fraction of C_2C_{12} myotubes binds [^{3}H]IP$_3$ with a K_d of 60.1 ± 22.2 nM and a maximal binding capacity of 2.80 pmol/mg of protein; the fit to the equilibrium binding curve implies a single type of receptor. *D*, [^{3}H]IP$_3$ binding to 1B5 cell homogenates. The K_d (61.8 ± 16.3 nM) and B_{max} (3.12 pmol/mg of protein) were determined by best fitting of data. The nonspecific binding were measured in the presence of 2 μM IP$_3$. The saturation isotherms were fitted to a single class of binding sites.

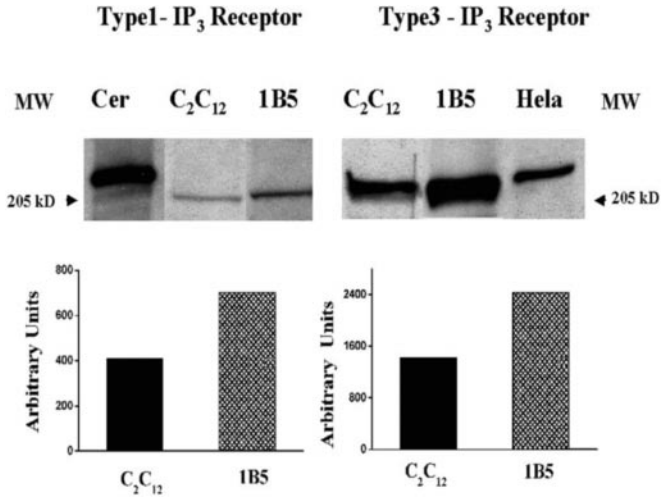

FIG. 6. **SDS-polyacrylamide gel analysis of type 1 and type 3 IP$_3$ receptor.** A representative record of at least three independent preparations is presented. Both type 1 (*left panel*) and type 3 (*right panel*) IP$_3$ receptor were visualized by Western blot analysis in total cell lysates of C_2C_{12} (first *lane*) and 1B5 (second *lane*) myotubes. Cerebellum proteins (first *lane*, *left panel*) and HeLa cells (*lane 3*, *right*) were used as standard for type 1 and type 3, respectively. Aliquots of these homogenates (10 μg) were analyzed on 7% SDS-polyacrylamide gel, and later the proteins were detected using commercial antibodies. Type 3 IP$_3$ immunoreactivity was higher in 1B5 cells as compared with total lysates obtained from C_2C_{12}. *MW*, molecular mass.

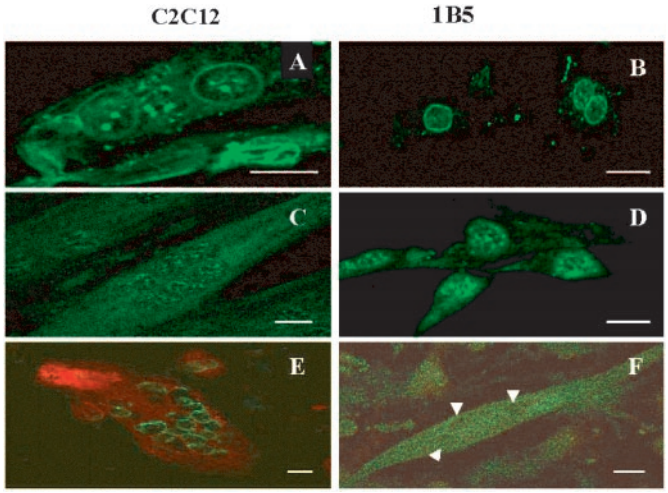

FIG. 7. **Immunocytochemistry.** Fluorescence immuno-labeling of types 1 and 3 IP$_3$ receptors in C_2C_{12} myotubes. *A* and *C*, epitope affinity-purified rabbit polyclonal antibody to IP$_3$R type 1 labels the nuclear envelope region and some internal nuclear structures; the latter label is nonspecific since preimmune serum labels only internal nuclear structures (6). On the other hand, antibody to type 3 IP$_3$R shows internal nuclear labeling (*C*). Myotubes show very faint fluorescence when incubated with the fluorescence-conjugated secondary antibody alone (not shown) or when incubated in the presence of the antigenic peptide (*F*); no nuclear label was detected in this case (*arrows*). Anti-ryanodine receptor, together with anti-type 1 IP$_3$R staining is shown in C_2C_{12} (*E*). A monoclonal antibody against ryanodine receptor was used. Type 1 and 3 IP$_3$ receptors in 1B5 myotubes with fluorescence immuno-labeling were also evident. *B* and *D*, the spatial distribution of these receptors was not different compared with control C_2C_{12} cells, but label intensity was usually higher. *Calibration bar* for all images is 15 μm.

immunoblotting polyacrylamide gel electrophoresis-separated total cell lysates (Fig. 6). Cerebellum proteins (*first lane*, *left panel*) and HeLa cells (third *lane*, *right panel*) were used as positive controls for type 1 and type 3 IP$_3$ receptors, respectively. Both C_2C_{12} and 1B5 cell myotubes co-expressed both type 1 and type 3 IP$_3$ receptor isoforms (Fig. 6) in nearly equal proportions. However, a densitometry analysis showed that 1B5 myotubes expressed higher levels of both proteins, which were estimated as a fraction of total protein compared with C_2C_{12} myotubes (Fig. 6, *lower panels*).

Immunocytochemistry—The intracellular localization of IP$_3$ receptor isoforms was monitored by immunofluorescence labeling and confocal microscopy. As shown in Fig. 7, *A* and *B*, fluorescence due to type 1 IP$_3$R presents a similar pattern in both C_2C_{12} and 1B5 myotubes. Immunoreactivity is seen primarily in the nuclear envelope and some internal nuclear structures. However, the internal nuclear labeling is most likely to be nonspecific because these structures are seen when the cells are incubated with preimmune serum in place of the primary antibody (6). The staining of type 1 IP$_3$ receptor appears to be continuous around the nuclear envelope. This was confirmed by sectioning the cells in *z* axis using scanning confocal microscopy (data not shown). On the other hand, the antibody against type 3 IP$_3$R shows a significant amount internal nuclear labeling (Fig. 7, *C* and *D*) especially in 1B5 myotubes, where it is expressed at high levels. There is also a punctate pattern of type 3 staining throughout the cellular matrix in both cell types. C_2C_{12} myotubes showed specific immunoreactivity after exposure to anti-RyR antibodies (Fig. 7*E*) and demonstrated that RyR, when expressed, did not co-localize with IP$_3$ receptor. This indicates that there is a different spatial distribution of these proteins in these myotubes. As

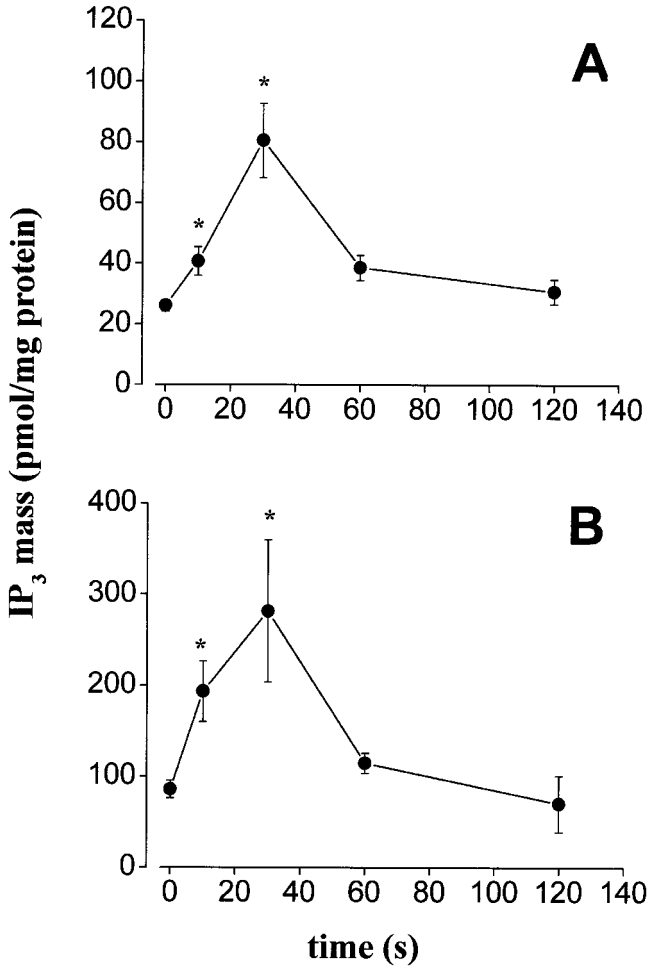

FIG. 8. **IP_3 mass in C_2C_{12} and 1B5 muscle cells line.** *A*, time course of IP_3 mass changes upon K^+ depolarization in C_2C_{12} myotubes. C_2C_{12} myotubes were preincubated for 20 min in resting solution and then depolarized with 47 mM K^+. IP_3 mass was measured in the soluble extract as described under "Materials and Methods." Each point represents the mean ± S.D. from three independent experiments performed in triplicate. *B*, time course of K^+ depolarization on intracellular IP_3 mass in 1B5 cells. The basal value of IP_3 mass increased significantly after 15 s of K^+ exposure and reached a maximum at 30 s. The IP_3 mass then gradually returned to its basal value by 120 s. The response is significantly different (*) when compared with basal values: $p < 0.05$.

expected, there was no RyR immunoreactivity in 1B5 myotubes (not shown). Rabbit preimmune serum was used to determine nonspecific labeling' no secondary antibody mark was evident under these conditions (Fig. 7*F*).

IP_3 Mass—The IP_3 mass was measured by a radioreceptor assay in both normal and dyspedic myotubes. The basal level of intracellular IP_3 in C_2C_{12} cells was 26.1 ± 1.9 pmol/mg of protein, and in dyspedic cells, the basal level was 2–3-fold higher (80.6 ± 9.7 pmol/mg of protein). When these results are expressed as pmol of IP_3 per million of cells counted, this difference still persists. The level of IP_3 in cultured muscle cells appears to be regulated by membrane potential; transient increases in the mass of IP_3 are elicited by potassium-induced depolarization (6, 9). When both C_2C_{12} and 1B5 myotubes were incubated with saline containing a high potassium concentration (Fig. 8), we observed that both responded to the rise in extracellular potassium by increasing their IP_3 mass. A peak of 3–3.5-fold higher than the basal value was reached 30 s after depolarization, but the mass of IP_3 was significantly higher than basal 10 s after depolarization. For C_2C_{12} the intracellular level of IP_3 increased to a maximum of 80.6 ± 12.2 pmol/mg of protein or 329% of the initial value after 30 s ($n = 7$, $p < 0.05$ *versus* initial value) and declined to 38.7 ± 4.1 pmol/mg of protein after 60 s ($p < 0.05$). The values were back to basal levels after 120 s. For 1B5 myotubes, the intracellular level of IP_3 first increased to a maximum of 281 ± 78 pmol/mg of protein or 348% of the initial value after 30 s ($n = 7$, $p < 0.05$ *versus* initial value) and then declined to 114.6 ± 11.1 pmol/mg of protein after 60 s ($p < 0.05$). As for C_2C_{12} cells, it returned again to basal values after 120 s. During the incubation of the cells with the resting solution, the basal level of intracellular IP_3 was not modified.

DISCUSSION

Our data show that in the absence of RyR expression, cultured dyspedic skeletal myotubes retain the slow delayed intracellular calcium transient that is seen as a second phase of release after a K^+ depolarization in normal myotubes expressing RyR. This slow delayed release appears to be due to the presence of IP_3 receptors that are expressed in both types of cells. Our experimental evidence to support this hypothesis include the following. 1) Myotubes from a normal muscle cell line like C_2C_{12} show fast and slow calcium signals that follow high potassium depolarization, as those described for myotubes in primary culture. 2) 1B5, dyspedic muscle cells, which do not express any of the ryanodine receptor isoforms (confirmed by [^{3}H]ryanodine binding and immunocytochemistry), show a calcium increase induced by K^+ depolarization that seems to be especially important at the level of the nucleus. The kinetics of this transient is compatible with the slow signal present in rat and mouse primary cultures (5, 6, 20) or C_2C_{12} cells. Both the fast calcium transient, which is responsible for excitation-contraction coupling, and the fast-slow wave, which is associated with signal propagation, are absent in 1B5 myotubes. The fast calcium signal is restored in these cells when RyR1, but not RyR3, is expressed (11, 13, 16). 3) Both [^{3}H]IP_3 binding and Western blot analysis show the presence of IP_3 receptors in both 1B5 and C_2C_{12} muscle cells. The presence of IP_3R isoforms was confirmed by immunocytochemistry. Type 1 IP_3Rs were localized preferentially in the nuclear envelope, and both type 1 and type 3 IP_3R immunoreactivity was higher in 1B5 cells compared with C_2C_{12}. 4) In both 1B5 and C_2C_{12} cells, K^+ depolarization resulted in an increase in IP_3 mass. The kinetics of the IP_3 mass transient is compatible with IP_3 release being the precursor to the calcium transient.

Binding studies confirm that IP_3Rs are more abundant than RyRs in cultured muscle cells, as has been previously reported (6, 9, 26). It would be interesting to know the relative amounts of the sub-types of IP_3Rs present in these cells. The higher staining of type 3 antibodies in Western blots is not a direct proof of higher antigen concentration, since the antibodies were directed against different epitopes and their avidity for the antigen is unknown. The binding studies likewise, do not directly address the matter. Values of K_d for the different isoforms reported in the literature are around 1 nM for type 1 (or 2) and about 40 nM for type 3 (29). The value we found by fitting our data to a single receptor type curve (our Scatchard plots, with a limited number of points, do not show a clear second component) is around 60 nM for both cell lines. So, if K_d values for IP_3Rs in muscle cells are comparable with those described for receptors purified from other cells, we may have a high proportion of type 3 IP_3R as compared with type 1 in our cells. Such a high type 3 receptor content could mask a small proportion of high affinity components in the Scatchard plot.

We have previously shown that K^+ depolarization produces a pattern of calcium signals on cultured skeletal muscle myotubes, characterized by a fast and a slow intracellular calcium increase (5, 6). We postulated that the fast response is dependent on ryanodine receptors, whereas the second, slow response

appears associated to cell nuclei and mediated by IP_3. The results of the present study support this hypothesis and demonstrate a functional role for IP_3 as a modulator of calcium-mediated cellular processes in the skeletal muscle cell, occurring on the time scale of seconds. The fact that the slow calcium signal can be inhibited by various substances known to interfere with either IP_3 generation or IP_3 action (24, 25) and the fact that these compounds do not interfere with the fast signals in C_2C_{12} cells provide further support in this direction. The lack of a fast calcium transient and the presence of a delayed, slow calcium transient seen in 1B5 myotubes is similar to what was seen in C_2C_{12} myotubes and (previously) in primary rat myotubes that were incubated with 25 μM ryanodine (6). In the myotubes pretreated with ryanodine, the fast calcium transient disappeared, but the slow calcium increase, especially the one at the level of the cell nuclei, remained. In normal myotubes, the slow calcium signal is usually seen as a propagated wave, progressing along the main axis of the myotube from nucleus to nucleus at speeds between 20 and 60 μm/s, depending of whether the cytosolic wave front or the nuclear peak calcium is considered. In ryanodine-treated primary myotubes, propagation does not occur that way, but as a sudden increase in calcium in both the cytosol and nuclei after a delay (6). Similarly, C_2C_{12} cells treated with ryanodine and 1B5 myotubes, which lack ryanodine receptors, also show this delayed but concerted increase of calcium in the whole cell, and this increase is especially notable as fluo-3 fluorescence changes in the cell nuclei. Thus, 1B5 cells appear to be the right model to test the hypothesis that ryanodine receptors are not involved in the generation of the slow calcium transient but do have a role in slow wave propagation. It is also interesting to note that the duration of the calcium transient in any given spot of the cell is significantly shorter for normal untreated cells than either the signal measured in the presence of ryanodine in normal cells or the signal in untreated dyspedic cells. This fact could be interpreted in favor of a role for ryanodine receptors in the turn-off of the calcium transient and, thus, contribute to the generation of an oscillatory pattern as the product of cross-talk between ryanodine receptors and IP_3 receptors.

It is interesting to speculate on the possible function for slow calcium transients in muscle cells. Our primary hypothesis, supported by the fact that potassium depolarization triggers both extracellular signal-regulated kinases 1 and 2 and cAMP-response element-binding protein phosphorylation in primary culture,[2] is that these signals could be caused by a privileged communication pathway from the surface membrane to the nucleus to regulate gene transcription. There is also support for this hypothesis by work using other cell types (Refs. 30–32, reviewed in Ref. 33). A second possibility is that these signals are intended to regulate local Ca^{2+} concentration within the cell. Whatever the mechanism, the existence of this signal certainly suggests the presence of different calcium release compartments in muscle cells, the nuclear envelope being one of them (7, 32, 34). The precise role of the subtypes of IP_3 and ryanodine receptors in what appears to be a complex time and space signaling pattern remains to be established.

Acknowledgment—M. Estrada thanks Comisión Nacional de Investigación Científica y Tecnológica (CONICYT) for a graduate student fellowship.

REFERENCES

1. Franzini-Armstrong, C., and Jorgensen, A. O. (1994) *Annu. Rev. Physiol.* **56,** 509–534
2. Meissner, G. (1994) *Annu. Rev. Physiol.* **56,** 485–508
3. Melzer, W., Hermann-Frank, A., and Lüttgau, H. Ch. (1995) *Biochim. Biophys. Acta* **1241,** 59–116
4. Rios, E., and Pizarro, G. (1991) *Physiol. Rev.* **71,** 849–908
5. Jaimovich, E., and Rojas, E. (1994) *Cell Calcium* **15,** 356–368
6. Jaimovich, E., Reyes, R., Liberona, J. L., and Powell, J. A. (2000) *Am. J. Physiol.* **278,** C998–C1010
7. Guihard, G., Proteau, S., and Rousseau, E. (1997) *FEBS Lett.* **414,** 89–94
8. Humbert, J. P., Matter, N., Artault, J. C., Köppler, P., and Malviya, A. N. (1996) *J. Biol. Chem.* **271,** 478–485
9. Liberona, J. L, Powell, J. A., Shenoi, S., Petherbridge, L., Caviedes, R., and Jaimovich, E. (1998) *Muscle Nerve* **21,** 902–909
10. Buck, E. D., Nguyen, H., Pessah, I. N., and Allen, P. D. (1997) *J. Biol. Chem.* **272,** 7360–7367
11. Fessenden, J. D., Wang, Y., Moore, R. A., Chen, S. R., Allen, P. D., and Pessah I. N. (2000) *Biophys. J.* **79,** 2509–2525
12. Kiselyov, K. I., Shin, D. M., Wang, Y., Pessah, I. N., Allen, P. D., and Muallem, S. (2000) *Mol. Cell* **6,** 421–431
13. Moore, R. A., Nguyen, H., Galceran, J., Pessah, I. N., and Allen, P. D. (1998) *J. Cell Biol.* **140,** 843–851
14. Nakai, J., Dirksen, R. T., Nguyen, H. T., Pessah, I. N., Beam, K. G., and Allen, P. D. (1996) *Nature* **380,** 72–75
15. Protasi, F., Franzini-Armstrong, C., and Allen, P. D. (1998) *J. Cell Biol.* **140,** 831–842
16. Protasi, F., Takekura, H., Wang, Y., Chen, S. R., Meissner, G., Allen, P. D., and Franzini-Armstrong, C. (2000) *Biophys. J.* **79,** 2494–2508
17. Ward, C. W., Schneider, M. F., Castillo, D., Protasi, F., Wang, Y., Chen, S. R. W., and Allen, P. D. (2000) *J. Physiol.* (*Lond.*) **535,** 91–103
18. Minta, A., Kao, J. P. Y., and Tsien, R. Y. (1989) *J. Biol. Chem.* **264,** 8171–8178
19. Castleman, K. (1989) *Digital Image Processing*, Englewood Cliffs, Prentice-Hall, New Jersey
20. Estrada, M., Liberona, J. L., Miranda, M., and Jaimovich, E. (2000) *Am. J. Physiol.* **279,** E132–E139
21. Jaimovich, E., Donoso, P., Liberona, J. L., and Hidalgo, C. (1986) *Biochim. Biophys. Acta* **855,** 89–98
22. Ramos-Franco, J., Fill, M., and Mignery, G. A (1998) *Biophys. J.* **75,** 834–839
23. Bredt, D. S., Mourey, R. J., and Snyder, S. H. (1989) *Biochem. Biophys. Res. Commun.* **59,** 976–982
24. Gafni, J., Munsch, J. A., Lam, T. H., Catlin, M. C., Costa, L. G., Molinski, T. F., and Pessah, I. N. (1997) *Neuron* **19,** 723–733
25. Maruyama, T., Kanaji, T., Nakade, S., Kanno, T., and Miroshiba, K. (1997) *J. Biochem.* **122,** 498–505
26. Liberona, J. L, Caviedes, P., Tascón, S., Hidalgo, J., Giglio, J. R., Sampaio, S. V., Caviedes, R., and Jaimovich, E. (1997) *J. Muscle Res. Cell Motil.* **18,** 587–598
27. Berridge, M. J. (1993) *Nature* **361,** 315–325
28. Ferris, C. D., and Snyder, S. H. (1992) *Annu. Rev. Physiol.* **54,** 496–488
29. Wojcikiewicz, R. J. H, and Luo, S. G (1998) *Mol. Pharmacol.* **53,** 656–662
30. Dolmetsch, R. E., Xu, K., and Lewis, R. S. (1998) *Nature* **392,** 933–936
31. Li, W., Llopis, J., Whitney, M., Zlokarnik, G., and Tsien, R. Y. (1998) *Nature* **392,** 936–941
32. Stehno-Bitel, L., Luckhoff, A., and Clapham, D. E. (1995) *Neuron* **14,** 163–167
33. Bading, H. (2000) *Eur. J. Biochem.* **267,** 5280–5283
34. Gerasimenko, O. V., Gerasimenko, J. V., Tepikin, A. V., and Petersen, O. H. (1996) *Pflügers Arch. Eur. J. Physiol.* **432,** 1–6